Ion Conductivity in a Magnesium Borohydride Ammonia Borane Solid-State Electrolyte

PCCP

Tuning the interface adhesion of Ag/ZnO composites by doping ZnO with metallic ions: A DFT study

Journal:	*Physical Chemistry Chemical Physics*
Manuscript ID	CP-ART-04-2022-001911
Article Type:	Paper
Date Submitted by the Author:	26-Apr-2022
Complete List of Authors:	Chen, Zi-Yao; Harbin Institute of Technology Shao, Wenzhu; Harbin Institute of Technology, School of Materials Science and Engineering Li, Wei-Jian; Yantai University Sun, Xueyin; Harbin Institute of Technology, Zhen, Liang; Harbin Institute of Technology, School of Materials Science and Engineering Li, Yang; Harbin Institute of Technology

PCCP
Physical Chemistry Chemical Physics

Guidelines for Reviewers

Thank you very much for your agreeing to review this manuscript for *Physical Chemistry Chemical Physics (PCCP)*.

PCCP is an international journal for the publication of cutting-edge original work in physical chemistry, chemical physics and biophysical chemistry, spanning experiment, theory, computation and data science. To be suitable for publication in *PCCP*, articles must include significant innovation and/or insight into physical chemistry; this is the most important criterion that reviewers and the Editors will judge against when evaluating submissions. Further information on our scope can be found at rsc.li/pccp.

PCCP's Impact Factor is **3.676** (2020 Journal Citation Reports®)

The following manuscript has been submitted for consideration as a

PAPER

Full papers should contain original scientific work that has not been published previously. Full papers based on Communications are encouraged provided that they represent a substantial extension of the original material. There are no restrictions on the length of a paper. Authors should include a brief discussion in the Introduction that sets the context for the new work and gives their motivation for carrying out the study.

When preparing your report, please:

- Focus on the originality, importance, impact and reliability of the science. English language and grammatical errors do not need to be discussed in detail, except where it impedes scientific understanding.
- Use the journal scope and expectations to assess the manuscript's suitability for publication in *PCCP.*
- State clearly whether you think the article should be accepted or rejected and include details of how the science presented in the article corresponds to publication criteria.
- Inform the Editor if there is a conflict of interest, a significant part of the work you cannot review with confidence or if parts of the work have previously been published.

Best regards,

Professor David Rueda
Editorial Board Chair
Imperial College London, UK

Dr Michael A. Rowan
Executive Editor
Royal Society of Chemistry

Contact us

Please visit our reviewer hub for further details of our processes, policies and reviewer responsibilities as well as guidance on how to review, or click the links below.

What to do when you review

Reviewer responsibilities

Process & policies

Harbin Institute of Technology

Harbin • Weihai • Shenzhen

Dear Editors,

We are submitting a manuscript entitled "Tuning the interface adhesion of the Ag/ZnO composite by doping ZnO with metallic ions: A DFT study" for consideration as an ***article*** in ***Physical Chemistry Chemical Physics.***

Benefited from the excellent integrative performance, Ag/ZnO composites, have been widely investigated and applied in various fields, during which, the weak interface adhesion brought about the shortcomings of the Ag/ZnO composites like poor formability, weak wettability, brittleness, and the reduction of the transmission efficiency of electrons and ions. Despite the recent studies on improving the interface adhesion of the Ag/ZnO by advanced preparation technology, it requires more investigations on the metallic ionic doping effects to tune the interface adhesion of the Ag/ZnO intrinsically in atomic scale.

To deeply understand the doping effects on interface adhesion, DFT calculations have emerged as an indispensable tool, being able to single out factors correlated to the interface properties, to provide many useful insights at the atomic scale. As a promising semiconductor and photocatalysts, the functionalities, such as photocatalytic and electrical conductivity, of the modified ZnO by doping have been extensively studied by theoretical calculations and experiments. However, there were rarely studies on the interface adhesion of the Ag/doped ZnO composites.

In this work, we investigate the work of separation (W_{sep}), the bond-lengths and effective bond order of the interfacial bonds, electron orbitals hybridization and charge movement of the Ag/ZnO interfaces with various metallic ionic dopants under four typical orientation relationships by DFT (density functional theory) calculations. It is demonstrated that low-valence dopants could enhance the interface adhesion of the Ag/ZnO composites due to the formation of the Ag-O bond with higher covalency level and shorter bond-lengths induced by more efficient charge transfer and higher degree of the p-d hybridization between the interfacial Ag and O atoms.

Unexpectedly, Cu (iso-valence) and Al (high-valence) dopants also can improve the interface adhesion of the Ag(111)/ZnO($11\bar{2}0$). By analyzing the average effective bond order and the interface adhesion of the Ag(111)/ZnO($11\bar{2}0$) with various dopants, the existence of the Ag-M

bonds are found that can replace the Ag-O bonds to link Ag and ZnO slabs.

Moreover, we find that three atomic parameters (average of bond length, <*AEBO*>-the average of effective bond order, Δq-charge transfer) are able to quantificationally rationalize the W_{sep} (values of interface adhesion). With decreasing the valence states of the dopants, the <*AEBO*>, Δq, and the optimal W_{sep} values monotonous increase, as well as the average length of the Ag-O bond monotonous decreases.

This work establishes the relationship between bonding, electronic structure and interface adhesion of the Ag/ZnO, as well as provides deep insights into understanding of the doping effects on interface properties of the Ag/ZnO. These mechanisms may not only apply to tune the interface adhesion of the metal/oxide interfaces, but also inspire that of the metal/metal, organic/metal, heterogeneous junction interfaces.

The work described in this manuscript has not been published previously, nor is it under consideration elsewhere. All authors have agreed to submit this paper exclusively to the ***Physical Chemistry Chemical Physics***, and we hope you will find this article interesting and suitable for publication.

Thank you for considering our work!

Sincerely,

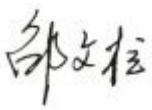

School of Materials Science and Engineering
Harbin Institute of Technology
92 West Dazhi Street, Harbin 150001, China
Tel: 86-451-86412133; fax: 86-451-86413921
E-mail: wzshao@hit.edu.cn

Tuning the interface adhesion of Ag/ZnO composites by doping ZnO with metallic ions: A DFT study

Zi-Yao Chen [a, b], Wen-Zhu Shao [a, b, *], Wei-Jian Li [c, *], Xue-Yin Sun [a, b, *], Liang Zhen [a, d], and Yang Li [a, d]

[a] *School of Materials Science and Engineering, Harbin Institute of Technology, Harbin 150001, China*

[b] *National Key Laboratory of Precision Hot Processing of Metals, Harbin Institute of Technology, Harbin 150001, China*

[c] *College of Nuclear Equipment and Nuclear Engineering, Yantai University, Yantai 264005, China*

[d] *MOE Key Laboratory of Micro-System and Micro-Structures Manufacturing, Harbin Institute of Technology, Harbin 150080, China*

[*]Corresponding authors: wzshao@hit.edu.cn (W.Z.S.), wjli@ytu.edu.cn (W.J.L.), hit2001sun@hit.edu.cn (X.Y.S.)

Abstract

Ag/ZnO composites have been widely applied, whilst their poor interface adhesion limits their integrative performance. Recently, doping has been considered as a versatile strategy to tune the interface adhesion of metal/ceramic interfaces, but the doping effect on interface adhesion and electronic structure needs to be further clarified. In this work, we investigated the interface adhesion and electronic structures of Ag/ZnO configurations with various dopants under four typical orientation relationships by density functional theory (DFT) calculations. We found that three atomic parameters (bond-lengths, <AEBO>-average of effective bond order, Δq-charge transfer) were able to quantitatively rationalize the W_{sep} (value to estimate of interface adhesion). For the Ag/ZnO (polar) interfaces, with increasing the valence number of dopants, the <AEBO>, Δq and W_{sep} increase monotonically, while the bond-lengths decreases monotonically. It demonstrated that p-type ZnO induced by low-valence dopants has larger charge transfer with Ag slabs and hence, to shorten the bond-lengths and increase the covalency level of the interfacial

Ag-O bonds, resulting in better interface adhesion of Ag/ZnO. Unexpectedly, high-valence doping can also enhance the interface adhesion of Ag/ZnO (non-polar) interface. The investigation of interfacial bonding indicated that not only Ag-O bonds, but also Ag-M (doping metal) bonds of Ag/ZnO (non-polar) interface could link the Ag and ZnO slabs. This work advances the understanding of doping effect on the interface adhesion of Ag/ZnO interfaces that can be extended to other metal/ceramic interfaces.

Keywords:
Ag/ZnO composites
DFT calculations
Doping with metallic ions
Interface adhesion
Electronic structure

1. Introduction

Benefited from the outstanding electrical conductivity, catalytic efficiency, thermal conductivity, and thermal stability, Ag/ZnO composites have been widely used in various fields, such as transparent conductive multilayer electrodes[1-3], photocatalysts[4-6], and electrical contact materials[7, 8]. Nevertheless, the weak interface adhesion brought about the shortcomings of Ag/ZnO composites like poor formability, weak wettability, brittleness, and the limited transmission efficiency of electrons and ions[9-11]. For example, Ag/ZnO electrical contact materials have been widely applied in the circuit breaker owing to the excellent thermophysical properties of ZnO, but the weak interface adhesion restricted to the resistance to arc-erosion of them[7, 8].

To improve the interface adhesion of Ag/ZnO electrical contact materials, gas atomization internal oxidation forging technology (AIOF)[8], chemical solution nano-coating[7], high energy ball-milling[12, 13] and other advanced composite preparation technology[14, 15] have been proposed. These techniques can improve the interface adhesion of Ag/ZnO composites at the mesoscale by enhancing the surface energy and activation of Ag and ZnO powders. Nevertheless, with the development of the electrical industry, due to the weak intrinsic interface adhesion between Ag and ZnO at the atomic-scale[16], the existing Ag/ZnO electrical contacts materials produced by above advanced technology have become difficult to meet the tougher service requirements to ensure the safety and stability of circuit.

Currently, modification of oxides by metallic ionic dopants has been considered as a versatile strategy to tune the interface adhesion of metal/oxide composites[7, 17-20]. To understand the doping effect on interface adhesion, density functional theory (DFT) calculations have emerged as an indispensable tool to single out factors correlated to the interface properties, and provide many useful insights at the atomic scale[21-27]. For example, Li et al.[17] have investigated adhesion and electronic structure of M-doped SnO_2/Cu configurations with three orientation relationships (M=Sb^{5+}, Mo^{6+}, Ti^{4+}, Zn^{2+} and Cu^{2+}), which indicated that low-valence doping (Cu^{2+} and Zn^{2+}) could motivate the formation of strong covalent bond, resulting in more stable interfaces. Similarly, Wang et al.[10] have investigated doping effect on interface adhesion of Ag(111)/ZnO(0001) interface. They also found that low-valence doping can enhance the total interfacial bond strengths due to reduction in charge on the interfacial O atoms, leading to enhancing the interface adhesion. Nevertheless, Shao et al.[28] have analyzed Mo-doped CaO(001)/Au(111) interface through DFT method and scanning tunneling microscopy. They demonstrated that the high-valence doping (substitution of Mo^{6+} for Ca^{3+} ions) could also induce more charge transfer and improve the interfacial strength of CaO/Au. Even though the interface adhesion of metal/doped-oxide interfaces has been studied extensively, some fundamental mechanisms remain undiscovered. As a promising semiconductor and photocatalysts, ZnO has been extensively functionalized via doping to improve the photocatalytic and electrical conductivity theoretically and experimentally[29-32]. However, there were still few studies on the interface adhesion of Ag/doped ZnO composites.

In this work, the effect of various metallic ionic dopants (i.e. Li^+, Ag^+, Cu^{2+}, Al^{3+}, Ti^{4+}) on the interface adhesion of the Ag/ZnO configurations with four types of orientation relationships were investigated by DFT calculations. Through geometry optimization, the W_{sep} of four types Ag/ZnO configurations with various dopants was calculated. Moreover, the total charge density, charge density difference and density of states (DOS) of the Ag/doped ZnO interfaces were analyzed to reveal the effect of dopants on electronic structure. Furthermore, we quantified three atomic parameters of interfaces, including bond-lengths, <AEBO> and Δq, which revealed the mechanism of doping on interface adhesion and built the relationship between electronic structure and interface adhesion. This work provides a universal approach to design and investigate the adhesion properties of metal/metallic oxides interfaces, which is also looking forward to inspired tuning the interface adhesion of metal/metal, metal/organic, heterogeneous junction interfaces.

2. Calculation details and methods

All calculations are based on DFT with the Perdew–Burke–Ernzerhof function of the generalized gradient approximation (GGA-PBE)[33]. The plane-wave pseudopotential method is applied to the Cambridge Serial Total Energy Package (CASTEP) of the Materials Studio, using ultrasoft pseudopotentials[34, 35]. All configurations have a 12 Å vacuum space that was set to avoid interaction between the periodically repeated slabs[36, 37] and are optimized using an energy cut-off of 500 eV and a SCF tolerance of 2.0×10^{-6} eV/atom. Based on the convergence testing of Ag and ZnO unit cell optimization (**Fig. S1 and S2**), the optimized lattice parameters of Ag and ZnO are listed in **Table S1**, which are consistent with previous experimental and theoretical investigations[36, 37]. Regarding the number of the total layers and relaxed layers of each slab, on the one hand, bulk effect should be taken into account and three fixed layers were usually modeled[38-40]. On the other hand, the W_{sep} of Ag(111)/ZnO(0001) with various number of relaxed layers (**Table S2**) shows that two relaxed layers are enough to ensure the accuracy and efficiency of calculating W_{sep} of Ag/ZnO configuration. Thus, five atomic layers in each slab including two relaxed layers next to the interface and three fixed layers are modeled.

The lattice mismatch determines the consistency between the calculated results and experimental results when building interfacial configurations between two slabs [41, 42]:

$$f = \frac{l_s - l_e}{l_e} \tag{1}$$

where l_s is the lattice parameter of substrate (the harder phase ZnO) and l_e is the lattice parameter of epitaxial layer (the softer phase Ag) deposited on the substrate. The positive or negative values of lattice mismatch correspond to the tensile or compressive state of Ag.

W_{sep}, the universal value to estimate the interface adhesion of Ag/ZnO interface, is defined as follow[43]:

$$W_{sep} = \frac{E_{Ag/ZnO} - E_{Ag} - E_{ZnO}}{A} \tag{2}$$

where $E_{Ag/ZnO}$ is the total energy of relaxed Ag/ZnO interfaces, E_{Ag} and E_{ZnO} are the total energies of the isolated upper and lower slabs in their interface geometry, respectively, and A is the Ag/ZnO interfacial area. Although computational methods of interface adhesion have been developed over years, this approximation is only a qualitative description of the interface adhesion due to some unsolved problems. For example, if the E_{Ag} and E_{ZnO} are calculated by fixed isolated slabs in their

interface geometry, which will introduce elastic deformation into the W_{sep}, while those are calculated by full relaxation, which will introduce free surface energy. A larger absolute value of W_{sep} (negative) represents the stronger interface adhesion.

Geometry optimization is a process to calculate the maximum energy (absolute) of the configurations by relaxing interfacial atoms via iterated operation. To acquire the optimal W_{sep} more accurately and faster, the universal binding-energy relation (UBER) method has been employed to calculate the total energies of each configuration with different separation (d) between the Ag and ZnO slabs when all atoms are fixed and the approximate equilibrium separation (d_0) corresponds to the maximum total energy [17, 44]. If the distance between Ag and ZnO slabs are not in equilibrium, the iterations of optimizing process will increase significantly, and even do not converge. More importantly, the distance between two slabs has determined the moving space of surface atoms, which affects the interface adhesion. Therefore, to ensure the comparability of the interface adhesion with various dopants, each distance between Ag and ZnO slabs should be identified by UBER calculation before optimization. During the optimizing process, the positions of interfacial atoms are relaxed using the conjugated gradient formalism until the forces are smaller than 0.05 eV/Å and the lattice parameters are fixed. The electronic properties are calculated using (6×6×1) Monkhorst-Pack k-point grids.

The atomic charge is calculated by Mulliken Charges to evaluate the partial charge by the divide-and-conquer method. The Δq, a significant parameter of Ag/ZnO interfaces, driven by the difference in the work functions between Ag and ZnO slabs when they are brought in contact, is the charge difference between the charges of the superficial O atoms in the ZnO configurations and the charges of the interfacial O atoms in the Ag/ZnO configurations.

3. Results and discussion

3.1. Configurations of Ag/ZnO interfaces

To investigate the interface properties of Ag/ZnO interfaces, the interfacial configurations should be first determined. Numerous theoretical and experimental studies have demonstrated that ZnO(0001) polar plane binds with metal better due to the surface charge compensation effect[45], such as Ag and Cu[10, 46], especially O-terminated ZnO(0001) surface[37, 38, 47]. It should be noted that

O-terminated ZnO(0001) plane could bind with Ag(111) to create various interfacial configurations with different stacking sites. Here, we focus on three typical kinds of Ag(111)/O-terminated ZnO(0001) configurations (**Fig. S3a**), during which O atoms are located on the top of Ag atoms in Z direction denoted as top sites, O atoms are projected on the middle of two Ag atoms denoted as bridge sites, and O atoms are projected on the triangle center of three Ag atoms denoted as hollow sites[48]. The W_{sep} of the above three kinds of configurations as a function of the separation between the Ag and ZnO slabs is calculated by the UBER method[49] (**Fig. S3b**), which shows that the Ag(111)/ZnO(0001) with hollow sites is most adhesive with the highest W_{sep} (**Fig. 1a and e**).

According to previous studies[50], the Ag(111) plane rotated by 30° (R30) deposited onto ZnO(0001) surface was observed by X-ray diffraction measurements and two of the shortest lattice vectors in the Ag(111) plane were almost coherent with √3 times of the shortest lattice vectors in the ZnO(0001) plane[37, 38, 47]. In order to compare the difference of the interface adhesion of the Ag/ZnO configurations with different lattice mismatches, a (2×√3) (R30) Ag(111)/ZnO(0001) configuration with a lattice mismatch of 2.9% is modeled, as shown in **Fig. 1b and f**.

Through extensive theoretical and experimental research, it is found that Zn- terminated ZnO($000\bar{1}$) and O-terminated ZnO(0001) always appear in pairs for bulk wurtzite ZnO[29], which is positive and negative charge, respectively[51]. Since O-terminated ZnO tends to link with Ag well, the O-terminated ZnO($000\bar{1}$) slab with neutral charge will be considered here as a comparison with the O-terminated ZnO(0001) on the difference of polarity. Also, we consider other three types of Ag(111)/ZnO($000\bar{1}$) configurations with different stacking sites, and the UBER curves are calculated, as shown in **Fig. S4**. Unlike the Ag(111)/ZnO(0001) configuration with hollow sites is the most adhesive, the Ag(111)/ZnO($000\bar{1}$) configuration with hollow sites has the lowest adhesion energy, since the Zn atoms located on the top of Ag atoms tend to be mutually exclusive. Whereas, the Ag(111)/ZnO($000\bar{1}$) configuration with top sites has the largest adhesion energy and is modeled as shown in **Fig. 1c and g**.

Except for the polar surfaces (ZnO(0001) and ZnO($000\bar{1}$)), non-polar surfaces account for 80% of the total exposure surfaces in polycrystalline ZnO, which may mainly determine the weak

interface adhesion of metals/ZnO interfaces[52]. To evaluate the doping effect on interface adhesion of Ag/ZnO(non-polar), a typical non-polar surface ZnO($11\bar{2}0$) consisting of a stoichiometric amount of oxygen and zinc atoms at the top is considered, and the Ag(111)/ZnO($11\bar{2}0$) configuration is modeled in **Fig. 1d and h**. Based on preliminary analysis and calculations, above four configurations with different orientation relationships are modeled in **Fig. 1**.

3.2. Interface adhesion

To compare the effect of various metallic ionic dopants on the interface adhesion of Ag/ZnO composites, each configuration with various dopants should be modeled, and the elements, doping behaviors, valence states, doping position of dopants should be confirmed first. Based on the semiconductor theory, holes (free ions) could be released in ZnO when low-valence (high-valence) doping, act as charge carriers convert the doped ZnO to an p-type (n-type) semiconductor. To compare the effect of different valence dopants on the interface adhesion, five typical metallic ions dopants (Li^+, Ag^+, Cu^{2+}, Al^{3+}, Ti^{4+}) whose valence state from +1 to +4, respectively, are chosen as the candidates to investigate doping effect. According to the previous study[53-55], these dopants are doped into ZnO by substituting the superficial Zn atoms to build each Ag/M-doped ZnO interface.

To evaluate the effect of doping on the interface adhesion of Ag/ZnO interfaces, the optimal W_{sep} of the four configurations with different dopants are calculated as shown in **Fig. 2.** It shows that the W_{sep} of all configurations with Ag^+ and Li^+ doping is higher than that without doping, which suggests that low-valence doping can enhance the interface adhesion of Ag/ZnO interfaces. Before the geometry optimization, the UBER curves of each Ag/ZnO interface with various dopants and the corresponding d_0 are calculated, as shown in **Fig. S5.** As shown in **Fig. 2**, comparing with the W_{sep} without doping, the W_{sep} of each configuration with Ag^+ and Li^+ doping is increased, while those with Cu^{2+}, Al^{3+} and Ti^{4+} doping are decreased, which can be found that the W_{sep} highly relies on the valence state of ions, except those of Ag(111)/ZnO($11\bar{2}0$) configuration. Depending on the difference of valence state, relative to the host ion (Zn^{2+}), above dopants can be classified as low-valence (i.e. Ag^+ and Li^+) (red columnar), iso-valence (i.e. Cu^{2+}) (blue columnar) and high-valence (i.e. Al^{3+} and Ti^{4+}) (yellow columnar). Consequently, it is suggested that zinc oxide based p-type semiconductors have a better interfacial bonding with Ag, which has a similar

conclusion to Cu/doped SnO_2 interfaces[17].

As shown in **Fig. 2**, the W_{sep} with each dopant in Ag(111)/ZnO(0001) configuration are higher than those in (2×√3) Ag(111)/ZnO(0001) configuration, because the elastic energy induced from the larger lattice mismatch in the former configuration increases the calculated W_{sep} away from the ideal W_{sep}[37, 50]. Since each configuration with various dopants has the same lattice parameters, the trends of both W_{sep} as a function of the dopant valence number are consistent.

The optimal W_{sep} of the Ag(111)/ZnO($000\bar{1}$) configuration with various dopants is lower than those of the Ag(111)/ZnO(0001) configuration; likewise, both trends of W_{sep} as a function of the dopant valence number are consistent. The W_{sep} of Ag(111)/ZnO(0001) and Ag(111)/ZnO($000\bar{1}$) configuration without doping is comparable to the other work (**Table S3**) [21, 47]. Besides, the differences in interface adhesion between these configurations have been found by mechanical testing of Ag/ZnO/Ag multilayers[21, 47]. As seen in **Fig. 1**, since polarity is the accumulating dipole moment produced by the surface of alternating parallel stacked layers of opposite charges, based on the distance between the surface O and Zn layer, the polarity of ZnO(0001) slab (1.93 Å) is stronger than that of ZnO($000\bar{1}$) slab (0.72 Å)[51]. In addition, the calculated results show that the Δq of the interfacial Ag-O bonds in Ag(111)/ZnO(0001) and Ag(111)/ZnO($000\bar{1}$) interface are 0.3 e and 0.04 e, respectively. Therefore, because of the difference of atomic geometry between ZnO(0001) and ZnO ($000\bar{1}$) slabs, the ZnO(0001) slab with the stronger polarity makes more compensating charge transferring towards Ag slab, resulting in the higher interface adhesion of Ag(111)/ZnO(0001) configuration with various dopants. Except for the Zn-O bond-length and dopants, the total charge of ZnO slabs may also affect the interface adhesion. To explore this effect, the configuration of Ag(111)/ZnO(0001) and Ag(111)/ZnO($000\bar{1}$) with non-neutral and neutral charge ZnO slabs are calculated and shown in **Fig. S6**, showing that the charge effect of ZnO slab on interface adhesion has much less influence than the doping effect (**Table S4**). The W_{sep} of non-neutral slab is larger, because some extra compensating charge transferred towards Ag slab is induced by non-zero dipole moment due to the ZnO slabs with non-neutral charge[56].

To investigate the difference between the polar and non-polar surface in ZnO, as shown in **Fig. 2**, the optimal W_{sep} of Ag/ZnO($11\bar{2}0$) is lower than that of Ag/ZnO (polar), which is

rationalized by the surface charge compensation effect due to polarity. Specifically, due to the instability of O atoms on the surface of polar ZnO, when formats the interface with Ag slab, the O atoms will gain electrons from Ag to fill their band based on the difference in electronegativity, which increases the charge transfer and enhances interface adhesion[45]. Remarkably, as for Ag(111)/ZnO($11\bar{2}0$) configuration, Cu^{2+} and Al^{3+} possess iso-valence and higher valence state but play a positive role in enhancing the interface adhesion, which will be discussed in the next section.

3.3. Interface electronic structure

To build the relationship between bond-lengths and interface adhesion, a comparative study of the Ag-O bond-lengths of the Ag(111)/ZnO(0001) interfaces with various dopants is performed as shown in **Fig. 3a-f**. The results show that low-valence doping can shorter the bond-lengths of Ag-O bonds that is a feature of the stronger interface adhesion. Interestingly, all atoms in the optimal Ag(111)/M-doped ZnO(0001) configurations are immobile in the top view (**Fig. 3a-f**) relative to those in Ag(111)/ZnO(0001) configuration **in Fig. 1e**. These superficial atoms only move in Z direction and O atoms could form similar bonds with three Ag atoms, which demonstrates that this configuration with hollow site is most adhesive. After using the UBER method, the Ag-O bond-lengths of Ag(111)/ZnO(0001) are 2.291~2.324 Å, and that of the optimal Ag(111)/ZnO(0001) (**Fig. 3a**) are shorter (2.239~2.266 Å), which confirms that the configuration becomes more adhesive with higher W_{sep} through geometry optimization. By comparison, the trend of Ag-O bond-lengths is: Ti^{4+}-doped > Al^{3+}-doped > Cu^{2+}-doped > undoped > Ag^{+}-doped > Li^{+}-doped (**Fig. 3a-f**), which is the opposite of the order of corresponding optimal W_{sep}. Similarly, the lengths of Ag-O and Cu-O bonds in the Ag/SnO_2 and Cu/SnO_2 interfaces were also calculated by DFT calculations, which revealed that the weak adhesion of these interfaces is ascribed to long interfacial bonds, resulting in densification difficulty and brittleness for Ag/SnO_2 and Cu/SnO_2 composites[57-59]. In other words, bond-length is inversely proportional to the bond-energy, determines the interface adhesion and low-valence doping can improve the energy of Ag-O bonds by generating shorter Ag-O bonds.

To appraise the doping effect on the bonding of Ag/ZnO interfaces, all average bond-lengths of the Ag-O bonds in four configurations are calculated, as shown in **Fig. 3g**. Likewise, order of

average lengths of the Ag-O bonds in both (2×√3) Ag(111)/ZnO(0001) and Ag(111)/ZnO($000\bar{1}$) agree with the above relationship that iso-valence and high-valence doping increases the bond-lengths of Ag-O bonds in the interfaces. Unexpectedly, as for Ag(111)/ZnO($11\bar{2}0$) configuration, the average Ag-O bond-lengths with Cu^{2+} and Al^{3+} doping are both shorter than that without doping, which is different from other configurations. Besides, the Ag-O bond-lengths of this configuration with Ag^{+} doping is longer than those without doping, while the optimal W_{sep} with Ag^{+} doping is higher. In other words, the enhancement of the interface adhesion of Ag(111)/ZnO($11\bar{2}0$) configuration with various dopants cannot be only explained from the bond-lengths of Ag-O bonds, because there are other ways to bind Ag and ZnO slabs, which will be discussed later.

To get more details about the Ag-O bonds at the interface, the total charge density and charge density difference for Ag(111)/ZnO(0001) configuration with various dopants are shown in **Fig. 4.** It shows that higher charge density between Ag and O atoms and the stronger charge depletion around the superficial O atoms in Ag(111)/ZnO(0001) configuration with Li^{+} doping than those without doping, while those with Cu^{2+} and Al^{3+} doping are lower and weaker, which demonstrates that low-valence doping can promote the formation of the stable Ag-O bonds with higher covalency level, conversely, high-valence and iso-valence doping can weaken the Ag-O bonds. The contour plot magnitude for the total charge density is shown in **Fig. 4b-d**, via blue-red colour coding [0,0.5 $Å^{-3}$]. As shown in **Fig. 4a**, the slice across the interfacial Ag and O atoms so as to focus on the charge density and difference of interfaces. Among them, the charge density of the chemical bonds between Ag and O atom represents the bonding strength[60, 61]. Significantly, there is a higher charge density between the Ag and O atoms in Ag(111)/ZnO(0001) configuration with Li^{+} doping than that without dopant (**Fig. 4 b and c**), while a lower charge in Ag(111)/ZnO(0001) with Al^{3+} and Cu^{2+} doping (**Fig. 4d and e**). Recently, the quantitative characterization of the bond energy at M/Al_2O_3 (M=Cu, Al)[62] and M/TiO_2 (M=Pt, Pd)[63] were applied by DFT calculations and electron energy loss spectroscopy (EELS), which demonstrated that the interface adhesion relies on the bond energy at the interface. Thus, the results demonstrate that low-valence doping can improve the interfacial Ag-O bonds, leading to enhance the interface adhesion of Ag(111)/ZnO(0001) configuration.

In addition, the contour plot magnitude for the charge density difference is shown in **Fig. 4e-h**, via blue-red colour coding [-0.1,0.1] Å^{-3}. The charge density difference is a common approach to identify the type of bond, which can be defined as[42, 61]:

$$\Delta\rho(\gamma) = \rho_{\mathrm{Ag/ZnO}}(\gamma) - \rho_{\mathrm{Ag}}(\gamma) - \rho_{\mathrm{ZnO}}(\gamma) \quad (3)$$

where $\rho_{\mathrm{Ag/ZnO}}(\gamma)$ is the total charge density of Ag/ZnO interfacial system, $\rho_{\mathrm{Ag}}(\gamma)$ and $\rho_{\mathrm{ZnO}}(\gamma)$ represent the total charge density of isolated Ag and ZnO slabs, respectively. Based on this formula, the red and blue regions in atoms represent the charge accumulation and depletion, respectively. Hence, according to the nature of chemical bonds, we could intuitively compare the covalency level of each Ag-O bond with various dopants. Specifically, there are both charge depletion (green) and charge accumulation (red) regions around the O atoms in the Ag(111)/Li^+-doped ZnO(0001) interface, which is the typical characteristic of the bond with high covalency level in **Fig. 4g**. Obviously, there is less charge depletion regions around the O atoms in the undoped interface in **Fig. 4f**, thus indicating that low-valence doping is attained by improving the covalency level of interfacial Ag-O bonds to enhance the interface adhesion. On the contrary, fewer charge depletion regions around the O atoms in **Fig. 4h and i** indicates that Cu^{2+} and Al^{3+} doping decrease the covalency level of the interfacial Ag-O bonds in Ag(111)/ZnO(0001) interface, which is consistent with the results in Cu/Cu^{2+}-doped SnO_2 interface, where low-valence doping increased the covalency level of interfacial bonds between metal and metallic oxides[17].

To characterize the bonding strength quantitatively, we calculate the <AEBO>, the average bond population (Mulliken)[49] between the interfacial Ag atoms and all atoms in ZnO who can bond with Ag and is defined as[21]:

$$< AEBO >= \frac{1}{n}\sum_{Ag} population(Ag - O) + population(Ag - M) \quad (4)$$

where n is the bonding number of Ag and interfacial atoms, population (Ag-O) and population (Ag-M*)* are the effective bond order of Ag-O and Ag-M (metal) bonds, the values of zero indicates a perfectly ionic bond, while values greater than zero indicate increasing levels of covalency[49]. In addition, the partial average of effective bond order (<AEBO>$_p$) of Ag-O bonds and Ag-M bonds are calculated by the average of population(Ag-O) and population(Ag-M), respectively.

According to the formula (4), all <AEBO> of the four configurations with different dopants are calculated as shown in **Fig. 5a**. Remarkably, these trends resemble the behaviour of the corresponding optimal W_{sep} (**Fig. 2**), which suggests that the strength of every atomic bonding at

the interface should be considered as a contributor for kinds of interface adhesion. Obviously, the <AEBO> of Ag(111)/ZnO(0001) interfaces with various dopants is higher than that of ($2 \times \sqrt{3}$)Ag(111)/ZnO(0001) interfaces as the trends of their W_{sep}, which indicates that the larger elastic energy induced from the larger lattice mismatch of Ag(111)/ZnO(0001) interfaces will increase the covalency levels of interfacial Ag-O bonds. Besides, the <AEBO> of Ag(111)/ZnO($000\bar{1}$) interfaces is also lower than that of Ag(111)/ZnO(0001) interfaces as the trends of their W_{sep}. It indicates that the stronger polarity of ZnO(0001) makes more compensating charge transferring towards Ag slab due to the difference of atomic geometry between ZnO(0001) and ZnO ($000\bar{1}$) slabs, resulting in the higher covalency levels of interfacial Ag-O bonds of Ag(111)/ZnO(0001) interfaces. On the one hand, the <AEBO> of all configurations decrease monotonically with the increase of the dopant valence number, except that of the Ag(111)/ZnO($11\bar{2}0$) configuration, which quantitatively reveals that low-valence doping can increase the covalency level of Ag-O bonds to enhance the interface adhesion of Ag/ZnO(polar) interfaces. On the other hand, the non-monotonic trend of <AEBO> correspond to the trend of optimal W_{sep}, for Ag(111)/ZnO($11\bar{2}0$) configuration with Cu^{2+} doping and Al^{3+} doping. In other words, it is crucial that the <AEBO> can represent all the interfacial atomic bonds to evaluate corresponding interface adhesion, which has been focused as a popular parameter to investigate the effect of oxide type[21] and doping content[39] on interface adhesion of kinds of interfaces.

To understand the abnormal W_{sep} with Cu^{2+} (iso-valence) and Al^{3+} (high-valence) doping that are higher than without doping in Ag(111)/ZnO($11\bar{2}0$) configuration, the $<AEBO>_p$ of the Ag-O and Ag-M bonds with various dopants are shown in **Fig. 5b**. It shows that the $<AEBO>_p$ of the Ag(111)/ZnO($11\bar{2}0$) configuration with Cu^{2+} and Al^{3+} doping is higher than that without doping, which indicates that Cu and Al atoms form bonds with Ag atoms, supplying the mainly population to links the Ag and ZnO slabs. The same contribution can be observed from the $<AEBO>_p$ of Ag(111)/Ag^{+}-doped ZnO($11\bar{2}0$) interface. Their optimal interfacial configurations are shown in **Fig. S7,** which shows that the Ag, Cu, and Al doping atoms are closer to the Ag slabs than the Li and Zn atoms. On the one hand, the Ag atoms that tend to lose electrons prefer to link with the O atoms of p-type ZnO (low-valence doping) with hole carriers rather than n-type ZnO (high-valence

doping). On the other hand, the Ag atoms can link with the doped atoms of the n-type ZnO due to the surface in ZnO ($11\bar{2}0$) (non-polar) including O and Zn atoms with a stoichiometric ratio. Besides, because of the electronegativity equilibrium theory[64], namely, the difference of electronegativity between two atoms determines the bond strength of them, the trends of bond strength as follows: Ag-Al bonds > Ag-Cu-bonds > Ag-Zn-bonds (the ions electronegativity: Ag-1.333, Zn^{2+}- 1.336, Cu^{2+}-1.372, and Al^{3+}-1.513)[64]. Therefore, the results reveal that the high-valence metallic dopants with a large electronegativity difference with Ag may improve the interface adhesion owing to the formation of strong Ag-M bonds in Ag/ZnO (non-polar) interfaces, even if these dopants may weaken the Ag-O bonds. A similar trend, improving interface adhesion by high-valence doping, was found in Au/Mo^{6+}-doped CaO interface[28] by DFT calculations and scanning tunneling microscopy. In addition, the formation of the strong Sn-Co and Cu-Co bonds in the metal/alloy interfaces (Cu/Co^{2+}-doped Sn) has enhanced the interface adhesion by 17.7% as well[40]. Therefore, the <AEBO> is a fundamental parameter related to the bonding and interface adhesion, which is suitable for different configurations with various orientations. This fundamental understanding of the interface adhesion is a crucial step towards exploring the doping strategy to tune the properties of composites.

In addition to the doping effect, the difference in atomic structure between polar and non-polar surface ZnO also causes the different behaviour of W_{sep} of the Ag/ZnO interfaces along the series of dopants. Unlike the polar ZnO with only O atoms in the first layer and Zn atoms located in the second atomic layer far away from Ag atoms (**Fig. 1a-c**), the first layer in ZnO ($11\bar{2}$ 0) (non-polar) includes O and Zn atoms in a stoichiometric ratio (**Fig. 1d**), which is beneficial to form Ag-M bonds[65]. Thus, the adhesion strength of Ag/ZnO with polar surface is determined by Ag-O bonds across the interface, while the adhesion of Ag/ZnO with non-polar surface highly relies on the Ag-O and Ag-M bonds simultaneously.

To further reveal doping effect on interface adhesion, we must draw attention to the interatomic interactions and the motion of electrons. Taking the Ag(111)/ZnO(0001) for example, the Density of State (DOS) of interfacial atoms are investigated, as shown in **Fig. 6**. The results suggest that low-valence doping makes ZnO transformed into p-type semiconductors, increases the degree of the p-d hybridization of Ag and O atoms at the Ag/ZnO interface, and induces higher Δq

of interfacial atoms, leading to the enhancement of Ag-O bonds and interface adhesion. When comparing with the O 2p states (dash line) of ZnO(0001) surface without doping (**Fig. 6a**), the valence band maximum (VBM) with low-valence doping (Li^+) (**Fig. 6b**) shifts are toward Fermi level, which is representative of the p-type semiconductors with positive charge carrier induced by creating holes. On the contrary, the VBM with iso-valence doping (Cu^{2+}) (**Fig. 6c**) and high-valence doping(Ti^{4+}) (**Fig. 6d**) shifts are away from Fermi level, which is representative of the n-type semiconductors with negative charge carrier induced by excess free electrons. Moreover, in the energy range of -6 ~ 0 eV, the Ag 3d states overlap with the O 2p states of interfaces (solid lines), and the overlapped areas represent the degree of the p-d hybridization for Ag and O atoms, suggesting the covalency level of bonds. When comparing the **Fig. 6a** with **Fig. 6b**, in the energy range of -2.7~0 eV, the Ag 3d states of Ag(111)/Li^+-doped ZnO(0001) interface are higher than that of undoped Ag(111)/ZnO(0001) interface, which results in the larger overlap between 3d states of Ag and 2p states of O, revealing a higher degree of the p-d hybridization caused by low-valence doping. After comparison of **Fig. 6a** and **Fig. 6c**, in the energy range of -2.7~0 eV, the Ag 3d states of Ag(111)/Cu^{2+}-doped ZnO(0001) interface are lower than that of undoped, representing a lower degree of the p-d hybridization caused by iso-valence doping. As shown in **Fig. 6d**, there is negligible overlap of Ag(111)/Al^{3+}-doped ZnO(0001) interface in the energy of -2.7~0 eV, revealing a lower degree of the p-d hybridization caused by high-valence doping.

Secondly, the charge of the superficial O atoms in the ZnO(0001) configurations and the interfacial O atoms in the Ag(111)/ZnO(0001) configurations with various dopants are calculated, as shown in **Fig. 6e**, which suggests that all the O atoms capture electrons from Ag atoms during the process of forming the interfaces due to the lower charge of the interfacial O atoms (negative).The atomic charge is calculated by Mulliken Charges to evaluate the partial charge by the divide-and-conquer method[49, 66]. The Δq, a significant parameter of Ag/ZnO interfaces, driven by the difference in the work functions between Ag and ZnO slabs when they are brought in contact[67], is the charge difference between the charges of the superficial O atoms in the ZnO configurations and the charges of the interfacial O atoms in the Ag/ZnO configurations. As shown in **Fig. 6f,** the Δq of the Ag(111)/ZnO(0001) configuration with various dopants decreases monotonically with the increase of the dopant valence number, which indicates that low-valence doping can promote electron transfer from Ag to O atoms, improving the strength of Ag-O bonds.

With Li doping, these monovalent cations result in the formation of holes in the O 2p valence band, which makes electrons flow to the oxides to fill the holes and restore the -2 charge of O atoms[68]. This leads to a stronger surface dipole, resulting in higher Δq than that with undoped. As far as we know, the process of charge transfer is exactly how chemical bonds are made, and the amount of Δq directly determines the strength of this bond[24, 40, 53, 68, 69].

To intuitively illustrate the doping effect on the interface properties of Ag/ZnO(polar) interfaces, the four-data graphs showing the optimal W_{sep} (circle area) as a function of the <AEBO> (x-axis), average length of Ag-O bond (d, red y-axis) and Δq (blue y-axis) of Ag(111)/ZnO(polar) configurations with various dopants, are shown in **Fig. 7,** and more details are shown in **Table 1**. Surprisingly, the <AEBO>, Δq, and the optimal W_{sep} increase monotonically, while the average length of Ag-O bonds decreases monotonically with the decrease of the dopant valence number. It reveals that, upon low-valence metallic ionic doping, more Δq were induced across the Ag/ZnO (polar) interface, and hence, the adhesion strength of Ag/ZnO interface was significantly enhanced by Ag-O bonds with covalency character. Significantly, since only Ag-O bonds act as a bridge to link the Ag and ZnO slabs in Ag(111)/ZnO(polar), similar monotonic relationships beteween these parameters may apply to other metal/oxide(polar) or metal/ O-terminated oxide configurations.

To reveal the doping effect on interface adhesion of Ag/ZnO(non-polar) interface, some parameters of Ag(111)/ZnO($11\bar{2}0$) configurations with various dopants are shown in **Table 2**. Unfortunately, neither Ag-O bond length (d), <AEBO>, nor Δq can quantitatively rationalize the trends of optimal W_{sep} with increasing the dopants valence number. On the one hand, the numbers of Ag-O bonds (N_O) and Ag-M (N_M) bonds with various dopants are different. On the other hand, various Ag-M bonds have different effects on interface adhesion. For example, the W_{sep} of Li^+-doped Ag(111) ZnO($11\bar{2}0$) configuration is larger than that of Al^{3+}-doped, but the <AEBO> and Δq are lower than Al^{3+}-doped Ag(111) ZnO($11\bar{2}0$) configuration. It indicates that the interfacial bonds in Al^{3+}-doped Ag(111) ZnO($11\bar{2}0$) configuration have stronger p-d hybridization and more charge transfer than those in Li^+-doped Ag(111) ZnO($11\bar{2}0$) configuration, yet the total bonding strength in Al^{3+}-doped Ag(111) ZnO($11\bar{2}0$) configuration is lower. As mentioned above,

for Ag/ZnO(non-polar) interface, high-valence dopants can also improve the interface adhesion due to the formation of Ag-M bonds and the large electronegativity difference between Ag and dopants. In conclusion, low-valence doping can improve the interface adhesion of Ag/ZnO composites including polar and non-polar plane of ZnO, while high-valence doping can both enhance and weaken the interface adhesion of Ag/ZnO composites, which is determined by the ratio of Ag/ZnO(non-polar) interface and electronegativity difference between dopants and Ag.

4. Conclusions

In this study, the effect of various metallic ionic dopants on the interface adhesion and electronic structure of Ag/ZnO interfaces under four typical orientation relationships were investigated by DFT calculations. Comparing with the high-valence and iso-valence dopants, low-valence dopants could improve the interface adhesion of Ag/ZnO(polar) interfaces owing to the formation of the Ag-O bonds with higher covalency level and shorter bond-lengths, which was induced by larger Δq and a higher degree of the p-d hybridization between the interfacial Ag and O atoms. Unexpectedly, Cu (iso-valence) and Al (high-valence) dopants could enhance the interface adhesion of Ag(111)/ZnO($11\bar{2}0$) configuration. By comparison the $<AEBO>_p$, the existing Ag-Cu and Ag-Al bonds in this configuration can replace the Ag-O bonds to link Ag and ZnO slabs and cause the abnormal trend of W_{sep} with the increase of the dopant valence number. Moreover, we found that three atomic parameters (average of bond-lengths, <AEBO>, Δq) were able to quantitatively rationalize the W_{sep}. The <AEBO>, Δq, and the optimal W_{sep} of Ag(111)/ZnO(polar) interface increased monotonically when the dopant valence number decreases, while the average Ag-O bond-lengths decreased monotonically. This work establishes the relationship between the interface adhesion and electronic structure of Ag/ZnO composites, as well as provides deep insights into the understanding of doping effect on the interface properties of Ag/ZnO. These mechanisms may not only apply to tune the interface adhesion of metal/oxide interfaces, but also inspire that of metal/metal, organic/metal, heterogeneous junction interfaces.

Supplementary

More details are shown in the supplementary material as follows: (1) Test of the calculation parameters, including the cut-off energy, *k*-point, numbers of relaxed layer, the relative sites between Ag and O atoms at the interfaces. (2) the W_{sep} of Ag(111)/ZnO(0001) with various number of relaxed layers. (3) The UBER curves of four configurations with various dopants. (4) The comparison between present work and other work on the lattice parameters of Ag and ZnO, the W_{sep} of Ag(111)/ZnO(0001) and Ag(111)/ZnO($000\bar{1}$) configuration. (5) The optimal interfacial configurations of Ag (111)/ZnO($11\bar{2}0$) with various dopants. (6) The comparison between Ag(111)/ZnO(0001) and Ag(111)/ZnO($000\bar{1}$) under different charge property with various dopants on configurations, E_{Ag} and W_{sep}.

Author contributions

Zi-Yao Chen: Investigation, Conceptualization, Writing - Original Draft. **Wen-Zhu Shao:** Conceptualization, Funding acquisition, Supervision. **Wei-Jian Li:** Methodology, Writing - Review & Editing. **Xue-Yin Sun:** Software, Visualization. **Liang Zhen:** Project administration, Resources. **Li Yang:** Writing - Review & Editing, Visualization.

Conflicts of interest

There are no conflicts to declare.

Acknowledgement

This work was financially supported by, the National Natural Science Foundation of China (Nos. 51877048 and 51371072).

REFERENCES

1. D. R. Sahu, S. Y. Lin and J. L. Huang, *Applied Surface Science*, 2006, **252**, 7509-7514.
2. E. Ando and M. Miyazaki, *Thin Solid Films*, 2001, **392**, 289-293.

3. J. Yong, C. H. Xu and Q. L. Guo, *Trans. Nonferrous Met. Soc. China*, 2013, **23**, 180-192.
4. Y. Zheng, L. Zheng, Y. Zhan, X. Lin, Q. Zheng and K. Wei, *Inorganic Chemistry*, 2007, **46**, 6980-6986.
5. S. A. Ansari, M. M. Khan, M. O. Ansari, J. Lee and M. H. Cho, *Journal of Physical Chemistry C*, 2013, **117**, 27023-27030.
6. Y. Zheng, C. Chen, Y. Zhan, X. Lin, Q. Zheng, K. Wei and J. Zhu, *Journal of Physical Chemistry C*, 2008, **112**, 10773-10777.
7. Z. Wei, L. Zhang, T. Shen, Z. Qiao, H. Yang, X. Fan and L. Chen, *Journal of Materials Engineering and Performance*, 2016, **25**, 3662-3671.
8. C. P. Wu, D. Q. Yi, J. Li, L. R. Xiao, B. Wang and F. Zheng, *Journal of Alloys & Compounds*, 2008, **457**, 565-570.
9. Z. Lin and P. D. Bristowe, *Journal of Applied Physics*, 2009, **106**, 013520.
10. T. Wang and P. D. Bristowe, *Journal of Applied Physics*, 2018, **124**, 235304.
11. A. G. Evans, D. R. Mumm, J. W. Hutchinson, G. H. Meier and F. S. Pettit, *Progress in Materials Science*, 2001, **46**, 505-553.
12. P. B. Joshi, V. J. Rao, B. R. Rehani and A. Pratap, *Indian Journal of Pure & Applied Physics*, 2007, **45**, 9-15.
13. L. Y. Wang, *Journal of Alloys and Compounds*, 2014, **582**, 1-5.
14. Q. A. Drmosh, Y. Wajih, I. O. Alade, A. K. Mohamedkhair and Z. H. Yamani, *Sensors and Actuators B Chemical*, 2021, **388**, 129851.
15. B. Barman, S. K. Swami and V. Dutta, *Materials Science in Semiconductor Processing*, 2021, **129**, 105801.
16. T. Phongpreecha, J. D. Nicholas, T. R. Bieler and Y. Qi, *Acta Materialia*, 2018, **152**, 229-238.
17. W. J. Li, W. Z. Shao, Q. Chen, L. Zhang, Y. Han, B. A. Chen, Q. Wang and L. Zhen, *Physical Chemistry Chemical Physics*, 2018, **20**, 15591 – 16296.
18. G. Li, X. Fang, W. Feng and J. Liu, *Journal of Alloys & Compounds*, 2017, **716**, 106-111.
19. C. H. Xu, D. Q. Yi, C. P. Wu, B. Wang, H. Q. Liu and X. D. Lu, *Journal of Functional Materials*, 2008, **39**, 1306-1309.
20. D. Jeannot, J. Pinard, P. Ramoni, E. M. Jost, D. Jeannot, J. Pinard, P. Ramoni and E. M. Jost, *IEEE Transactions on Components Packaging & Manufacturing Technology Part A*, 1994, **17**, 17-23.
21. D. Corni, H. Wiame, B. Lecomte, J. Cornil and D. Beljonne, *ACS Applied Materials & Interfaces*, 2017, **9**, 18346-18354.
22. M. A. R. Catlow, *Surface Science*, 2004, **561**, 43-56.
23. O. I. Malyi, V. V. Kulish, K. Bai, W. Ping and C. Zhong, *Surface Science*, 2013, **611**, 5-9.
24. M. Yu and D. R. Trinkle, *J. Phys. Chem. C*, 2011, **115**, 17799-17805.
25. O. Neufeld and M. C. Toroker, *Journal of Chemical Theory & Computation Jctc*, 2016, **12**, 1572-1582.
26. G. Byzynsk, C. Melo, D. P. Volanti, M. M. Ferrer, A. F. Gouveia, C. Ribeiro, J. Andrés and E. Longo, *Materials and Design*, 2017, **120**, 363-375.
27. Wenhua Pu, Wei Xiao, Jianwei Wang, Xiaowu Li and L. Wang, *Materials and Design*, 2021, **198**, 109387.
28. X. Shao, S. Prada, L. Giordano, G. Pacchioni and H. J. Freund, *Angewandte Chemie International Edition*, 2011, **50**, 11525-11527.
29. B. Meyer and D. Marx, *Physical Review B*, 2003, **67**, 35403-35403.
30. C. Kqab, X. A, D. Az, A. Ml, A. Qw, E. Syl, B. Hl and F. Gw, *Ceramics International*, 2020, **46**, 1494-1502.
31. Z. Li, S. Sun, X. Xiao, B. Zheng and A. Meng, *Catalysis Communications*, 2011, **12**, 890-894.
32. Q.N. Xue, L.G. Wang, X.W. Huang, J.X. Zhang and H. Zhang, *materials and Design*, 2018, **160**, 131-137.
33. J. P. Perdew, K. Burke and M. Ernzerhof, *Physical Review Letters*, 1996, **77**, 3865--3868.
34. G. Sun, J. Kürti, P. Rajczy, M. Kertesz, J. Hafner and G. Kresse, *Journal of Molecular Structure Theochem*, 2015, **624**, 37-45.
35. P. J. D. Lindan, *Journal of Physics Condensed Matter*, 2002, **14**, 2717-2744.

36. H. X. Cheng, X. X. Wang, Y. W. Hu, H. Q. Song, J. R. Huo, L. Li and P. Qian, *Journal of Solid State Chemistry*, 2016, **244**, 175-180.
37. Z. Lin and P. D. Bristowe, *Phys.rev.b*, 2007, **75**, 229-239.
38. Y. W. Hu, J. R. Huo, L. Li, H. X. Cheng and X. X. Wang, *Journal of Solid State Chemistry*, 2016, **244**, 175-180.
39. D. Cornil, N. Rivolta, V. Mercier, H. Wiame and J. Cornil, *ACS Applied Materials & Interfaces*, 2020, 40838−40849.
40. P. Zhang, Y. Wang, W. Lei, Y. Zou and C. Lu, *ACS Applied Materials & Interfaces*, 2019, **11**, 24648-24658.
41. Ayers and E. John, *Heteroepitaxy of Semiconductors: Theory, Growth, and Characterization*, CRC Press, New York, 2007.
42. L. Chen, Y. Li, B. Xiao, Q. Zheng and Z. Wang, *Materials & design*, 2019, **183**, 108-119.
43. Y. Qi and L. G. Hector, *Physical Review B*, 2004, **69**, 1681-1685.
44. A. Banerjea and J. R. Smith, *Physical Review B*, 1988, **37**, 6632–6645.
45. J. Goniakowski and C. Noguera, *Physical Review B Condensed Matter*, 2002, **66**, 085417.
46. C. Noguera, *Journal of Physics Condensed Matter*, 2000, **12**, 367.
47. C. L. Phillips and P. D. Bristowe, *Journal of Materials ence*, 2008, **43**, 3960-3968.
48. D. Jiang and E. Carter, *Surface Science*, 2004, **570**, 167-177.
49. M. Segall, R. Shah, C. Pickard and M. Payne, *Physical Review B Condensed Matter*, 1996, **54**, 16317.
50. N. Jedrecy, G. Renaud, R. Lazzari and J. Jupille, *Physical Review B*, 2005, **72**, 195404.
51. O. Dulub, U. Diebold and G. Kresse, *Physical Review Letters*, 2003, **90**, 016102.
52. O. Dulub, L. A. Boatner and U. Diebold, *Surface Science*, 2002, **519**, 201-217.
53. Qiang Fu, Luis Cesar and Colmenares Rausseo, *ACS Applied Materials & Interfaces*, 2015, **7**, 27782-27795.
54. S. Hang, H. Y. He and B. C. Pan, *Acta Physica Sinica*, 2021, **61**, 157301.
55. C. Rhr, P. Hidalgo, R. Muccillo and D. Gouvea, *Applied Surface Science*, 2003, **214**, 172-177.
56. P. W. Tasker, *Journal of Physics C: Solid State Physics*, 1979, **12**, 4977-4984.
57. J. C. Chen, J. Feng, B. Xiao and K. H. Zhang, *Journal of Materials Science & Technology*, 2010, **26**, 49-55.
58. M. Law, X. F. Zhang, R. Yu, T. Kuykendall and P. Yang, *Small*, 2010, **1**, 858-865.
59. Y. Wang, Y. S. Cui, W. Z. Shao and L. Zhen, *Low Voltage Apparatus*, 2003, **4**, 3-7.
60. G. Lan, Y. Jiang, D. Yi and S. Liu, *Physical Chemistry Chemical Physics*, 2012, **14**, 11178-11184.
61. W. J. Li, W. Z. Shao, Q. Chen, X. H. Sui, Y. Han, B. A. Chen, Q. Wang and L. Zhen, *Journal of Applied Physics*, 2019, **125**, 225303.
62. J. F. Sanz, *J.phys.chem.b*, 2002, **106**, 11495-11500.
63. H. R. Chen, P. Li, N. Umezawa, H. Abe and J. H. Ye, *Journal of Physical Chemistry C*, 2016, **120**, 5549-5556.
64. K. Li and D. Xue, *Journal of Physical Chemistry A*, 2006, **110**, 11332-11337.
65. S. E. Chamberlin, *Surface structures of polar and non-polar metal oxides*, University Microfilms International, Ann Arbor,MI, 2011.
66. R. S. Mulliken, *J. Chem. Phys.*, 1955, **23**, 1833-1840.
67. Sanderson and T. R., *Science*, 1951, **114**, 670-672.
68. S. Prada, L. Giordano and G. Pacchioni, *Journal of Physical Chemistry C*, 2012, **116**, 5781-5786.
69. S. Prada, M. Rosa, L. Giordano, C. D. Valentin and G. Pacchioni, *Physical Review B*, 2011, **83**, 245314.

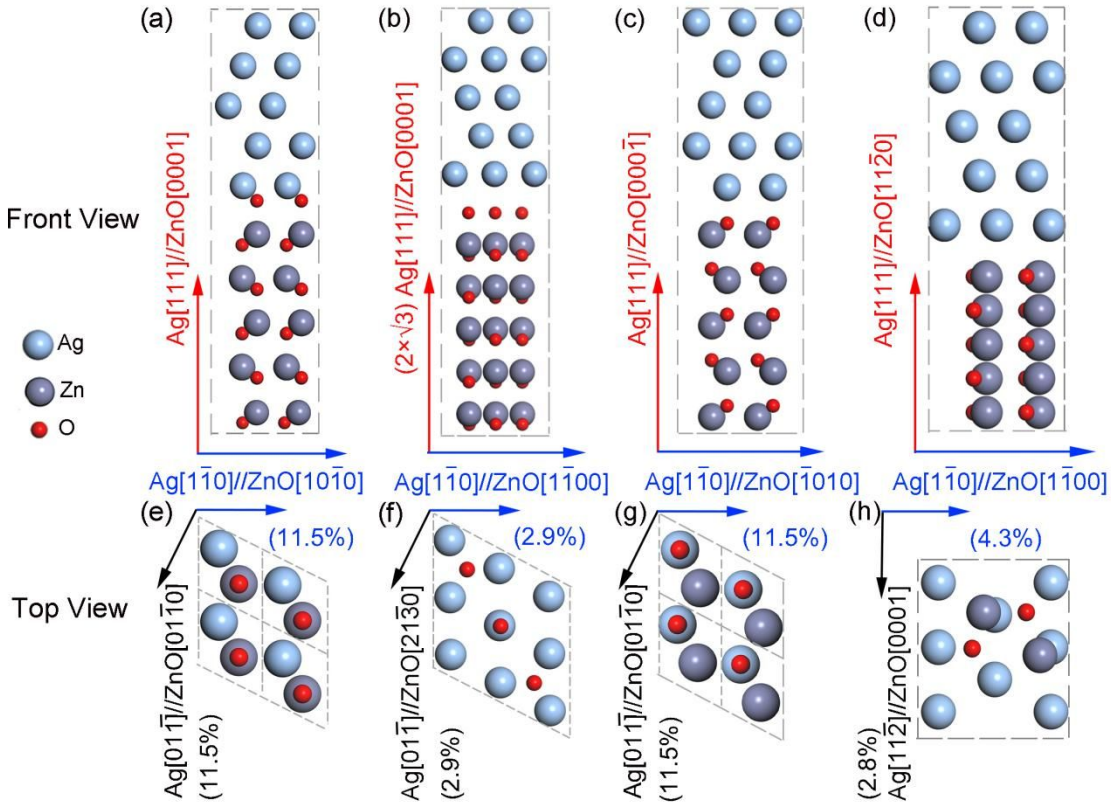

Fig. 1 Configurations of Ag/ZnO interfaces under different orientation relationships: (a, e) (1 × 1) Ag(111)/ZnO(0001), (b, f) (2×√3) Ag(111)/ZnO(0001), (c, g) (1 × 1) Ag(111)/ZnO(000 $\bar{1}$), and (d, h) (1 × 1) Ag(111)/ZnO(11 $\bar{2}$ 0) with O termination of ZnO. Related lattice mismatches and crystal orientations are shown along each direction. Upper row: front view. Lower row: top view of Ag/ZnO interface.

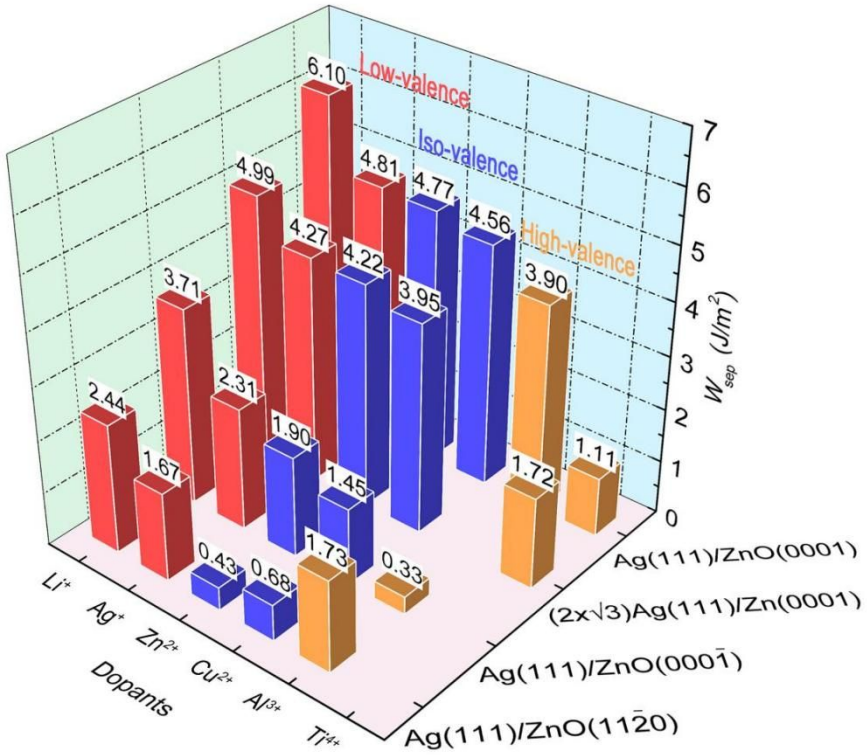

Fig. 2 The optimal W_{sep} values of Ag/ZnO configurations with different metallic ionic dopants under four typical orientation relationships: Ag(111)/ZnO(0001), (2×√3) Ag(111)/ZnO(0001), Ag(111)/ZnO(000$\bar{1}$), and Ag(111)/ZnO(11$\bar{2}$0) with O termination of ZnO. Compared with the valence state of the host ion (Zn^{2+}), the metallic ionic dopants in ZnO can be classified as low-valence (Ag^+ and Li^+) (red columnar), iso-valence (Cu^{2+}) (blue columnar) and high-valence (Al^{3+} and Ti^{4+}) (yellow columnar).

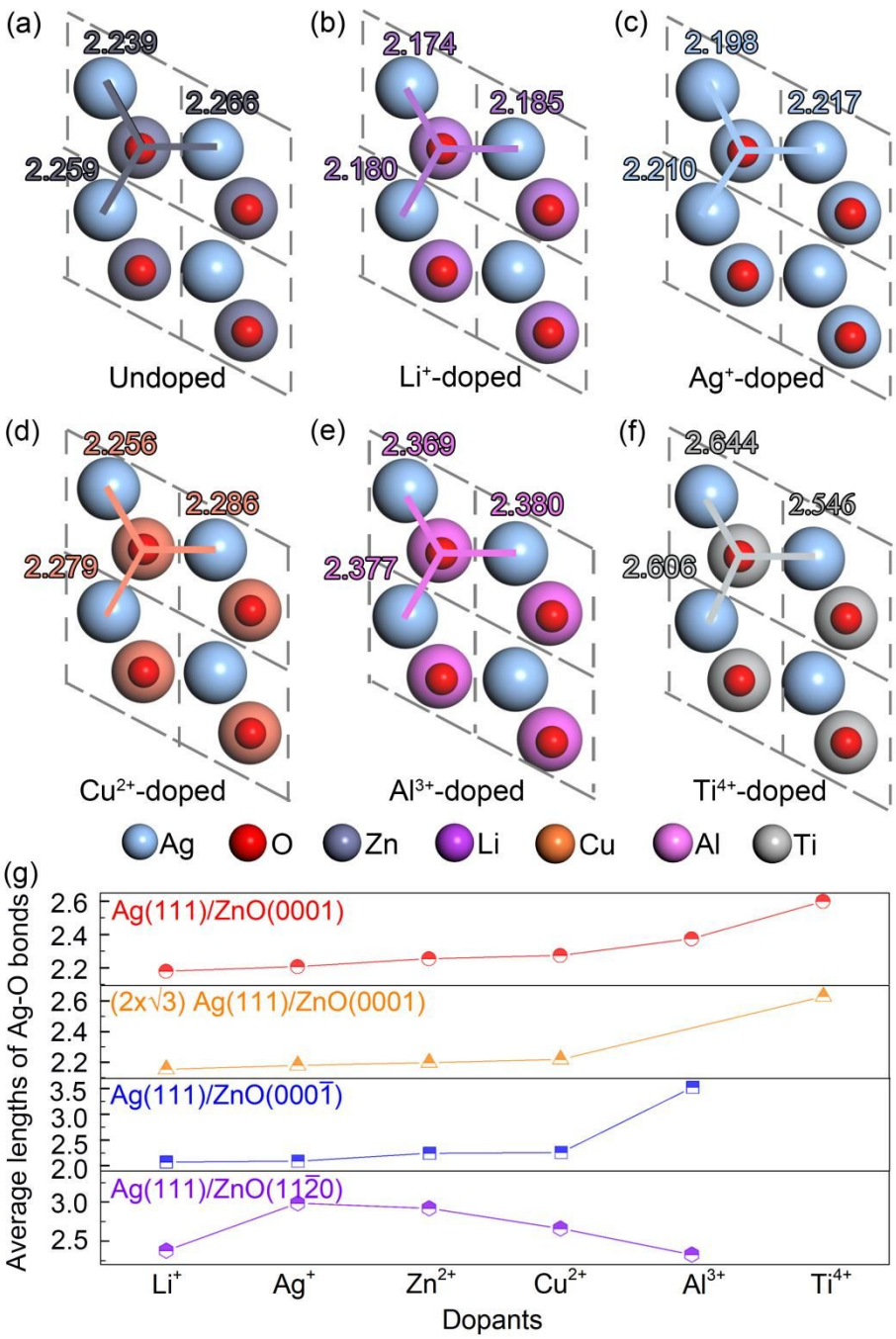

Fig. 3 (a-f) Top views of optimized (2×2) Ag(111)/ZnO(0001) configurations with different dopants and Ag-O bond-lengths (in units of angstrom): (a) Undoped, (b) Li^{+}-doped, (c) Ag^{+}-doped, (d) Cu^{2+}-doped, (e) Al^{3+}-doped and (f) Ti^{4+}-doped. (g) All average lengths of Ag-O bonds in four configurations with various dopants.

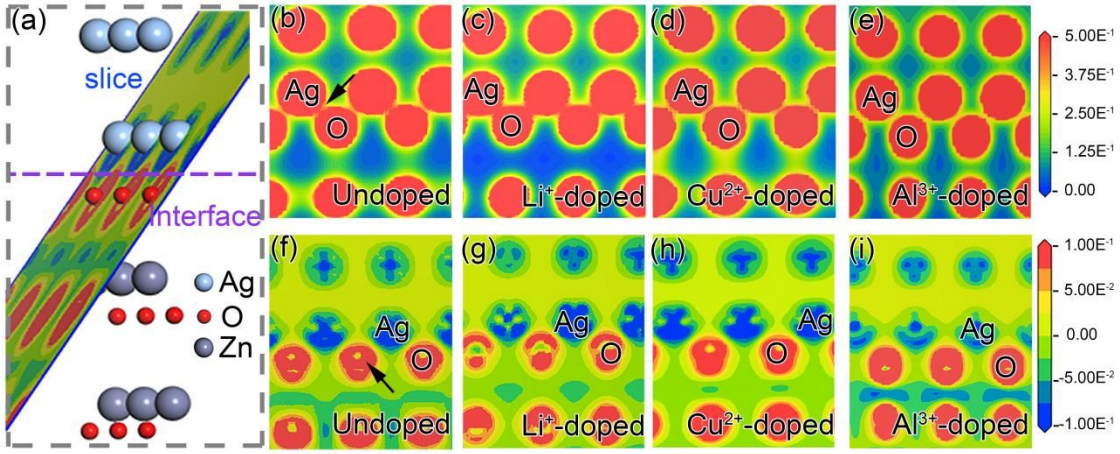

Fig. 4 Contour plots of the total charge density (b-e) andbute (f-i) for Ag(111)/ZnO(0001) configuration with different dopants (in units of $Å^{-3}$): (a) Schematic configuration shows the position of slice crossing the Ag and O atoms in the interface, the arrow represents the doping positions. (b, f) Undoped, (c, g) Li^{+}-doped, (d, h) Cu^{2+}-doped and (e, i) Al^{3+}-doped. The black arrows indicate the Ag-O bonds in the interfaces and the regions of charge depletion around the O atoms, respectively.

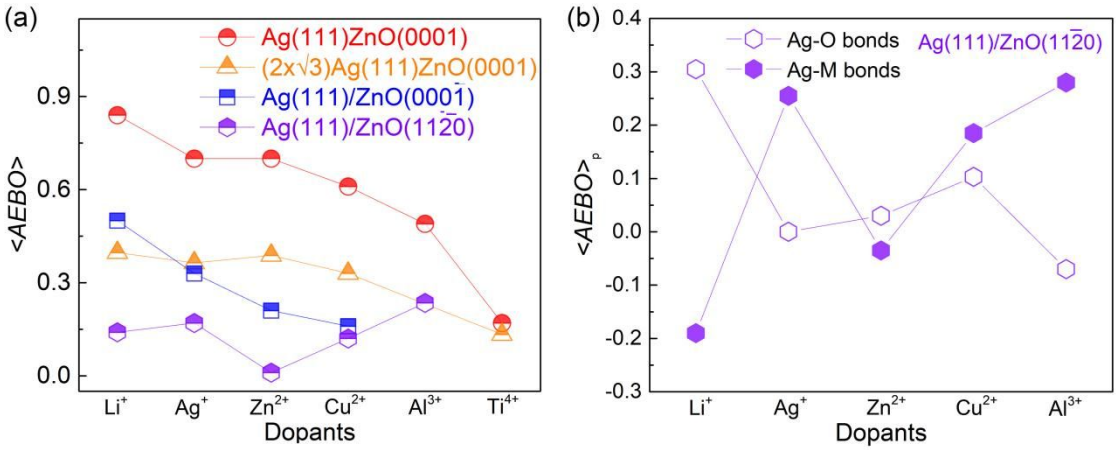

Fig. 5 (a) The average of effective bond orders(<AEBO>) of four configurations with different dopants and (b) the partial average of effective bond order ($<AEBO>_p$) of Ag(111)/ZnO(11$\bar{2}$0) configuration. Optimized interfacial configurations of the Ag (111)/ZnO(11$\bar{2}$0) with various dopants: (c) Li^{+}-doped, (d) Ag^{+}-doped, (e) Undoped, (f) Cu^{2+}-doped and (g) Al^{3+}-doped. Blue parallel lines represent the separation (h) between Ag and ZnO slabs.

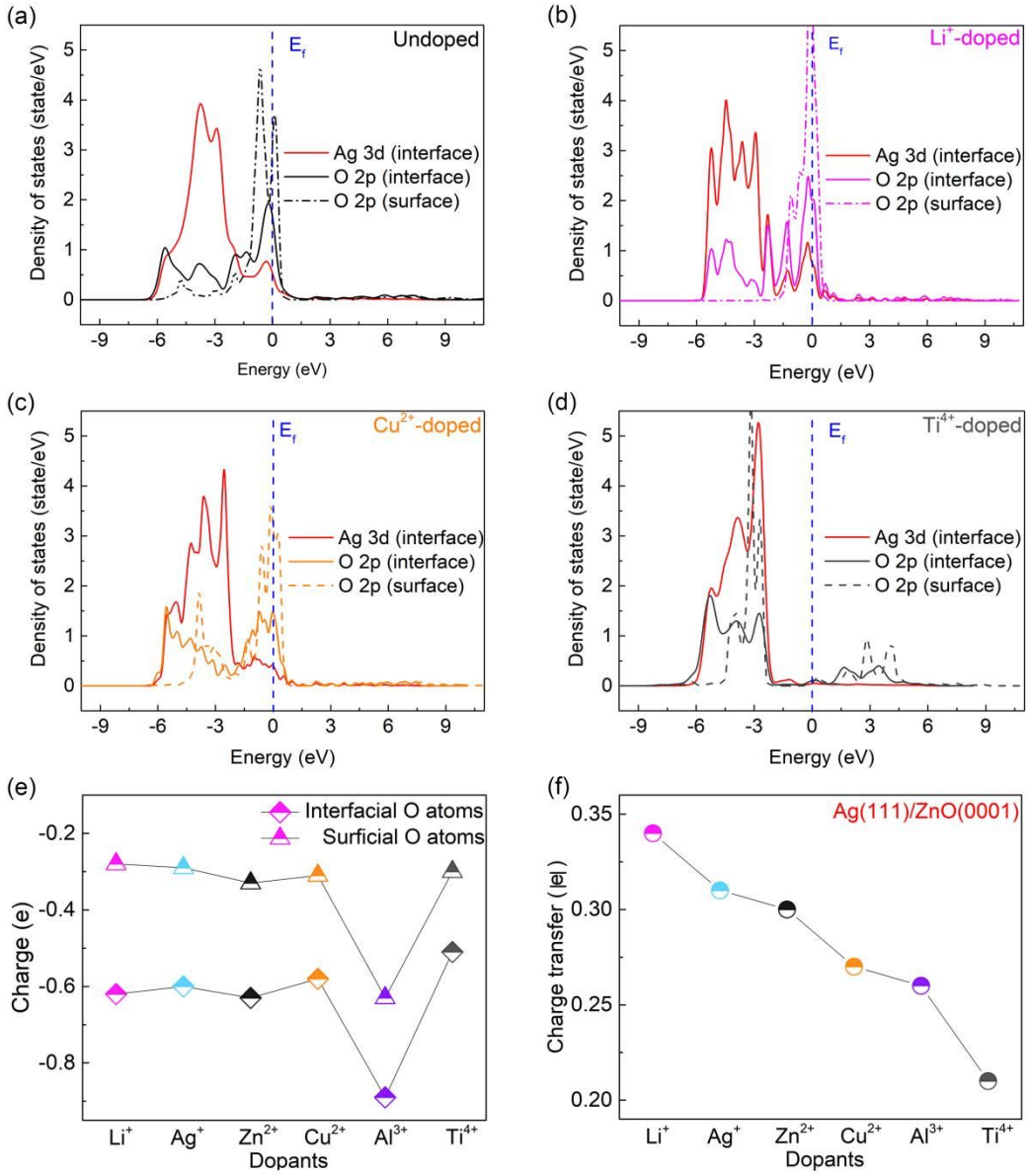

Fig. 6 (a-e) Density of states projected onto atoms at the Ag(111)/ZnO(0001) interfaces (solid line) and the ZnO(0001) surfaces (dash line) with different dopants: (a) Undoped, (b) Li^{+}-doped, (c) Cu^{2+}-doped, and (d) Ti^{4+}-doped. The vertical dash lines indicate the Fermi level. (e) The charge of O atoms at the ZnO(0001) surface and Ag(111)/ZnO(0001) interface with various dopants. (f) The charge transfer that forms the interface with various dopants.

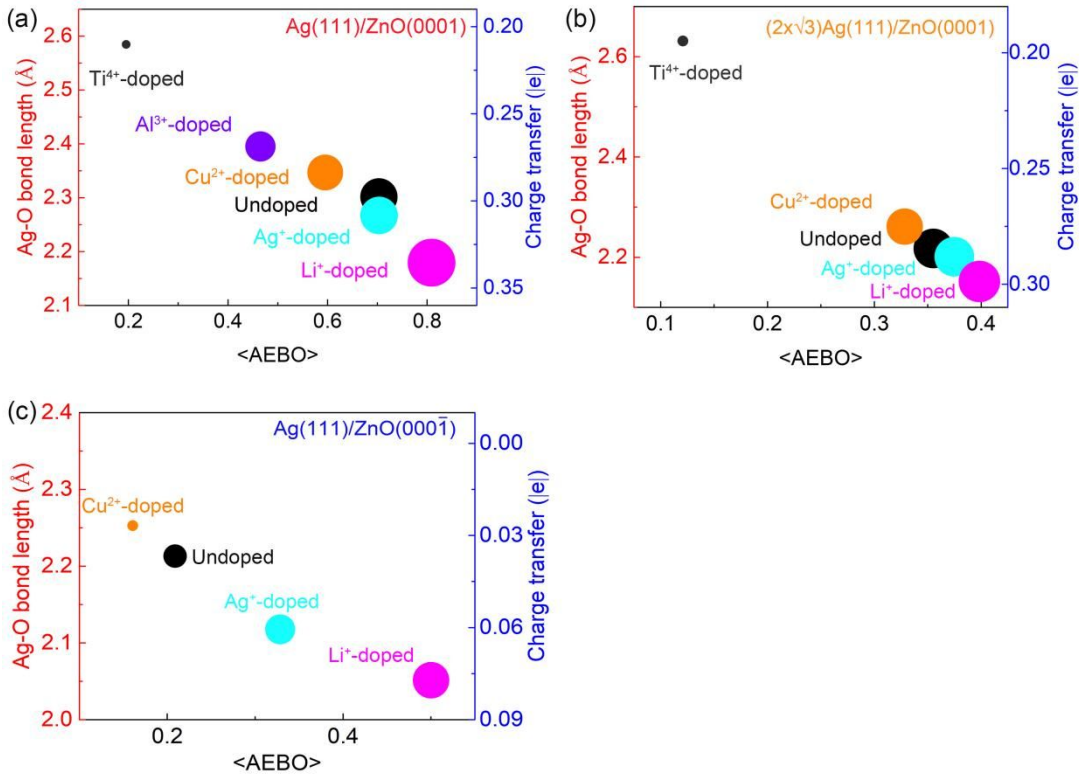

Fig. 7 Four-data graphs showing the optimal W_{sep} values (area of circle) as a function of <AEBO> (average of effective bond order) (x-axis), Ag-O bond length (red y-axis) and Δq (charge transfer) (blue y-axis) of Ag(111)/ZnO(0001) (a), (2×√3) Ag(111)/ZnO(0001) (b), and Ag(111)/ZnO(000 $\bar{1}$) (c) with various dopants.

Table 1 The Ag-O bond length (*d*), <AEBO> (average of effective bond order), Δq (charge transfer) and optimal W_{sep} values of Ag(111)/ZnO(polar) configurations with various dopants

	Dopants	*d* (Å)	<AEBO>	Δq (|e|)	W_{sep}(J/m^2)
Ag(111)/ZnO(0001)	Li^+	2.180	0.84	0.34	6.10
	Ag^+	1.208	0.7	0.31	4.81
	Zn^{2+}	2.255	0.7	0.3	4.77
	Cu^{2+}	2.274	0.61	0.27	4.56
	Al^{3+}	2.375	0.49	0.27	3.90
	Ti^{4+}	2.599	0.17	0.21	1.11
(2×√3)Ag(111)/ZnO(0001)	Li^+	2.155	0.40	0.300	4.99
	Ag^+	2.177	0.37	0.297	4.27
	Zn^{2+}	2.210	0.36	0.286	4.22
	Cu^{2+}	2.221	0.33	0.275	3.95
	Ti^{4+}	2.652	0.12	0.193	1.72
Ag(111)/ZnO(000$\bar{1}$)	Li^+	2.071	0.5	0.08	3.71
	Ag^+	2.088	0.33	0.06	2.31
	Zn^{2+}	2.243	0.21	0.04	1.9
	Cu^{2+}	2.257	0.16	0.03	1.45
	Al^{3+}	3.524	none	0	0.33

Table 2 The Ag-O bond length (d), <AEBO>, $<AEBO>_P$ of Ag-O bonds and Ag-M bonds, number of Ag-O bonds (N_O) and Ag-M bonds (N_M), Δq, and optimal W_{sep} values of Ag(111)/ZnO(11$\bar{2}$0) (non-polar) configurations with various dopants

Dopants	*d* (Å)	<AEBO>	$<AEBO>_p$ (Ag-O)	$<AEBO>_p$ (Ag-M)	N_O, N_M	Δq (|e|)	W_{sep} (J/m^2)
Li^+	2.378	0.140	0.305	-0.190	4, 2	0.35	2.44
Ag^+	2.985	0.170	0	0.255	1, 2	0.35	1.67
Zn^{2+}	2.920	0.002	0.03	-0.035	3, 2	0.12	0.43
Cu^{2+}	2.660	0.120	0.103	0.185	3, 2	0.18	0.68
Al^{3+}	2.997	0.235	-0.07	0.280	1, 3	0.38	1.73

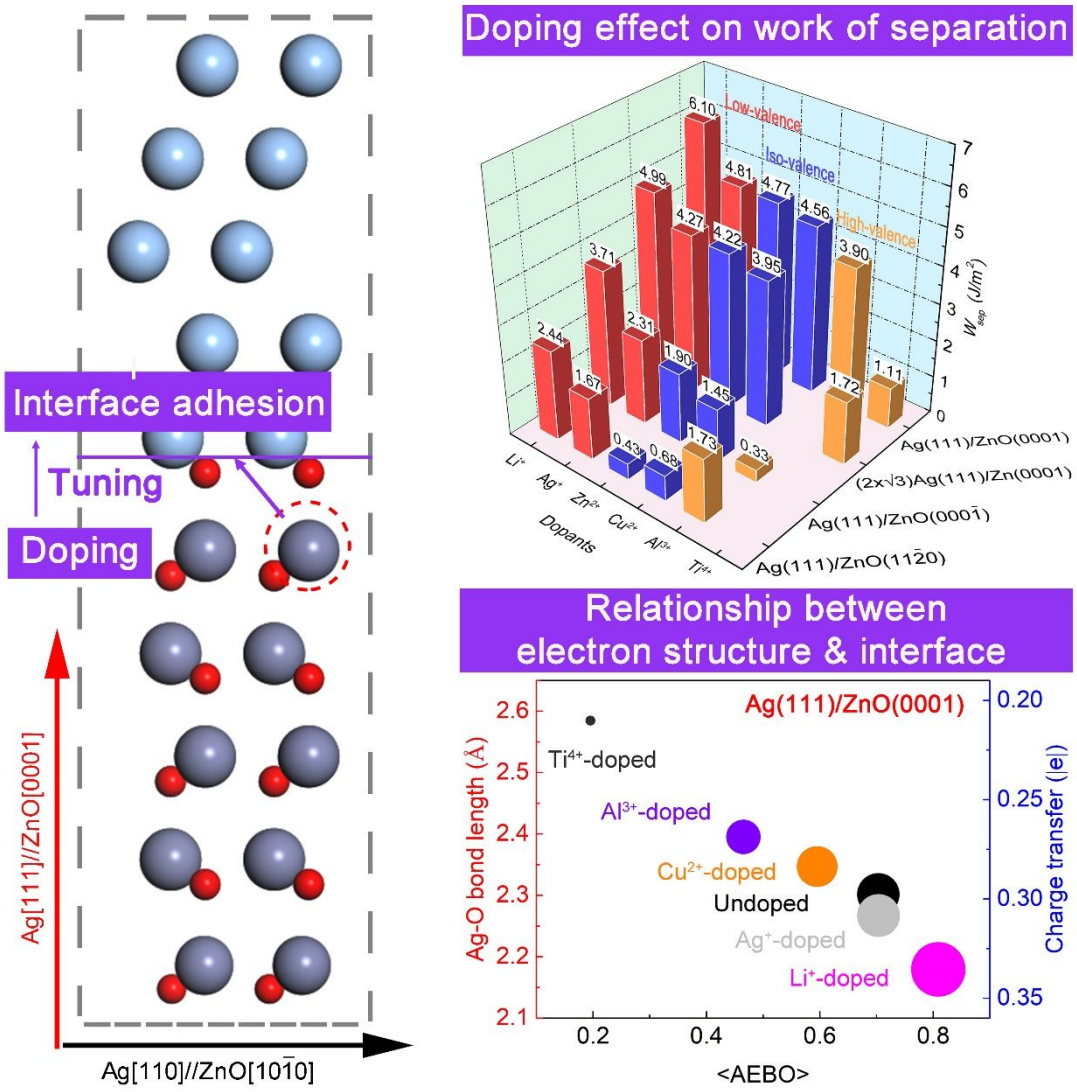
Interface adhesion
Tuning
Doping
Ag[111]//ZnO[0001]
Ag[110]//ZnO[10$\bar{1}$0]
Doping effect on work of separation
Low-valence
Iso-valence
High-valence
W_{sep} (J/m^2)
Dopants
Li$^+$
Ag$^+$
Zn^{2+}
Cu^{2+}
Al^{3+}
Ti^{4+}
Ag(111)/ZnO(0001)
(2x$\sqrt{3}$)Ag(111)/Zn(0001)
Ag(111)/ZnO(000$\bar{1}$)
Ag(111)/ZnO(11$\bar{2}$0)
Relationship between
electron structure & interface
Ag(111)/ZnO(0001)
Ti^{4+}-doped
Al^{3+}-doped
Cu^{2+}-doped
Undoped
Ag$^+$-doped
Li$^+$-doped
Ag-O bond length (Å)
Charge transfer (|e|)
<AEBO>